Proceedings of ICAD2006
4th International Conference on Axiomatic Design
Firenze – June 13-16, 2006
ICAD-2006-37

AXIOMATIC DESIGN OF NON-WETTING HEMOCOMPATIBLE SURFACES

Anthony J. Schrauth
schrauth@mit.edu
Massachusetts Institute of Technology
77 Massachusetts Avenue
Cambridge, MA 02139-4307
USA

Nam P. Suh
npsuh@mit.edu
Massachusetts Institute of Technology
77 Massachusetts Avenue
Cambridge, MA 02139-4307
USA

ABSTRACT

Biomedical devices implanted in the body, such as stents, must avoid the body's natural defense system in order to effectively perform their task. One of these natural defenses specific to blood is the clotting reaction. Any surface, implanted or externally used, that comes into contact with blood is considered an intruder, and the blood seeks to isolate the object by clotting on the foreign surface. The clotting process involves the identification of a foreign surface, the adsorption of proteins onto that surface, and then the agglomeration of platelets on the proteins to form a clot. The ability to resist the clotting of blood is very beneficial to device performance.

Since coagulation is a surface reaction, it is hypothesized that a reduction in the actual contact area between the blood and the surface should lead to dramatically reduced blood clotting. Axiomatic design is used to develop a structured surface to improve surface hemocompatibility. This research shows that the surface area reduction that results in super hydrophobic surfaces can be used to reduce blood coagulation on artificial surfaces. It is shown that appropriate surface structure, slender posts with a larger period relative to their width, can lead to extremely high apparent contact angles (θ^*=160°). Additionally, it is shown that the same surfaces significantly reduce platelet agglomeration in vitro under static blood.

Keywords: Axiomatic Design, Hemocompatibility, Structured Surfaces

1 INTRODUCTION

One of the many challenges involved in designing biomedical devices is the selection of materials that will interact successfully with biological systems. Adverse reactions to the biological environment can doom devices that perform exceptionally well in initial testing. For many devices, the specific problem is that of interacting with blood. These blood-handling biomedical devices can be implanted, such as stents or heart valves, or used externally, such as dialysis machines. The desire for hemocompatible materials for such applications has led to extensive research in the chemistry that drives blood-material interactions. Materials that prove successful are able to resist the development of blood clots, or thrombosis, for extended periods of time. In this paper an additional method to reduce blood clotting is proposed that uses surface geometry to eliminate as much of the blood-surface interaction as possible.

This paper presents a structured surface design based on rough wetting theory and Axiomatic Design concepts. The structured surface is manufactured and then put through preliminary tests for hemocompatibility.

2 BACKGROUND

Young's equation for the mechanical equilibrium of a sessile drop on a flat surface is central to any discussion on surface wetting properties.

$$\cos\theta = \frac{\gamma_{SV} - \gamma_{SL}}{\gamma_{LV}}. \quad (1)$$

It relates the surface energies (γ_{SV}, γ_{SL}, γ_{LV}) of the materials to the angle between the fluid-solid interface and the fluid-vapor interface (θ). Young's equation, however, is only valid for the ideal case of a solid surface that is smooth, rigid, homogeneous, and isotropic. Several researchers have investigated the effect that surface roughness and non-homogeneity have on the observed contact angle. Robert Wenzel developed a theory for rough surfaces based on the assumption that a fluid in contact with a rough surface completely wets the grooves in the surface (Figure 1a) [1,2]. As a result, the actual area of the solid liquid interface is greater than the apparent contact area—the actual contact area projected on the plane of the macroscopic surface. He defined a parameter called roughness ratio, *r*, which is the actual contact

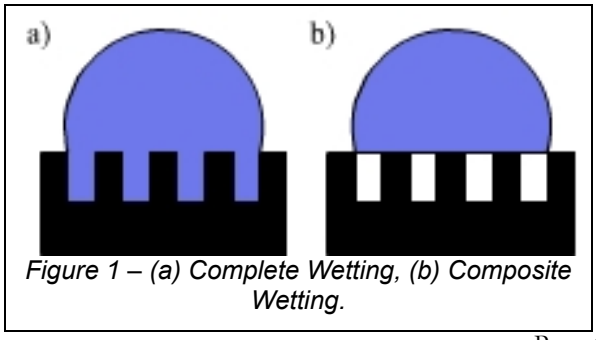

Figure 1 – (a) Complete Wetting, (b) Composite Wetting.

area between the fluid and the solid divided by the apparent contact area. The roughness ratio, *r*, takes values greater than unity. Consequently, a small increase in the apparent contact area, *dA*, leads to an increase in actual solid-liquid interfacial area of *rdA* and an equal decrease in actual solid-vapor interfacial area. This makes the change in surface free energy of the solid *r*-times greater than the perfectly smooth case. Consequently, Young's equation becomes

$$\cos\theta^* = \frac{r(\gamma_{SV} - \gamma_{SL})}{\gamma_{LV}} = r\cos\theta, \quad (2)$$

where θ^* is the apparent contact angle. It is clear that an increase in roughness will increase θ^* for $\theta > 90^\circ$ and will decrease θ^* for $\theta < 90^\circ$.

Cassie and Baxter used a similar formulation to investigate the effect that heterogeneous surfaces have on apparent contact angle [3]. They modeled a heterogeneous surface as being composed of two materials, one with an equilibrium contact angle of θ_1, and one with an equilibrium contact angle of θ_2. The area fraction of the surface with $\theta=\theta_1$ is defined to be ϕ_1 and the area fraction with $\theta=\theta_2$ is defined to be ϕ_2, where $\phi_1+\phi_2=1$. Substituting θ_1 and θ_2 into Young's Equation, we see that a small increase in wetted area, *dA*, leads to a change in surface free energy of the solid equal to $\phi_1\gamma_{lv}\cos\theta_1 + \phi_2\gamma_{lv}\cos\theta_2$. The equation for the apparent contact angle on the heterogeneous surface then becomes $\cos\theta^* = \phi_1\cos\theta_1 + \phi_2\cos\theta_2$, this is the Cassie-Baxter equation for heterogeneous surfaces.

This can be adapted to rough surfaces if we assume that the fluid does not wet the valleys of the surface, but only sits on top of the peaks. Referred to herein as the composite wetting case (Figure 1b). In this case, ϕ_s is defined to be the area fraction of the surface that is wetted, i.e. the area of the peaks in contact with the water divided by the total apparent contact area. Setting θ_2 to be 180° (the 'contact angle' of water with its vapor), ϕ_1 to be ϕ_s, and ϕ_2 to be 1-ϕ_s, it is found that

$$\cos\theta^* = \phi_s(\cos\theta + 1) - 1. \quad (3)$$

This is the Cassie-Baxter Equation for wetting of a rough surface. Under this formulation, the apparent contact angle increases for $\theta > 90^\circ$, but when $\theta < 90^\circ$ the composite wetting assumption cannot hold because capillary forces will pull the fluid into the valleys rather than keeping it on top of the peaks.

In both rough wetting theories, the apparent contact angle is determined by two parameters, one geometric parameter (ϕ_s or *r*) and one material parameter—the equilibrium contact angle, θ. In the Wenzel case, the apparent contact angle is very sensitive to the material contact angle, and as the roughness ratio, *r*, increases, so does the sensitivity to material contact angle. Consequently, a very large roughness ratio is required in order to get a large apparent contact angle when the material's contact angle is slightly larger than 90°, but as the material contact angle increases, the required roughness ratio becomes more achievable (Figure 2). In the Cassie-Baxter theory, the apparent contact angle is fairly insensitive to material contact angle over the range of area fraction, ϕ_s. Additionally, the apparent contact angle becomes less and less sensitive to material contact angle as the area fraction, ϕ_s, approaches zero (Figure 3). Consequently, the geometric parameter (ϕ_s) in the Cassie-Baxter theory has more control over the apparent contact angle independent of the original contact angle. This means that the acceptable range of material contact angles at a given area fraction, ϕ_s, is large, allowing for more material flexibility to achieve a given apparent contact angle. It also makes the system insensitive to changes in material contact angle due to imperfections and contamination.

Research seeking to develop hydrophobic materials has been pursued for the better part of a century. Early uses for hydrophobic materials were dominated by the desire to create waterproof coatings. As time passed, more potential uses for hydrophobic materials were presented. The results of much of this work (Teflon, for instance) have been integrated into our daily lives with great commercial success even though they offer contact angles up to only 110°. Even higher contact angles promise revolutionary new applications so an extensive body of research has developed in the field of creating so called superhydrophobic surfaces. Several groups have had success in creating surfaces by a variety of methods, yet most have used surface geometry to increase contact angles, since it appears chemical improvements have reached their limits.

A group at the Kao Corporation created super hydrophobic surfaces in 1996 using a fractal structure [4]. They created surfaces by solidifying mixtures of Alkylketene dimer (AKD) and dialkylketone (DAK). Controlling the ratio of AKD and DAK controls the fractal geometry and therefore the wetting behavior.

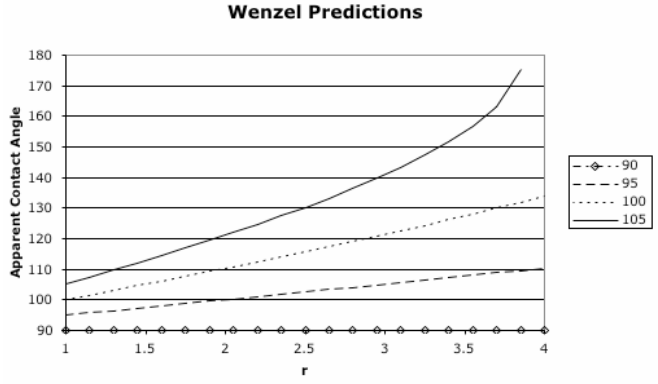

Figure 2 – Wenzel predictions for apparent contact angle as a function of the roughness ratio (r).

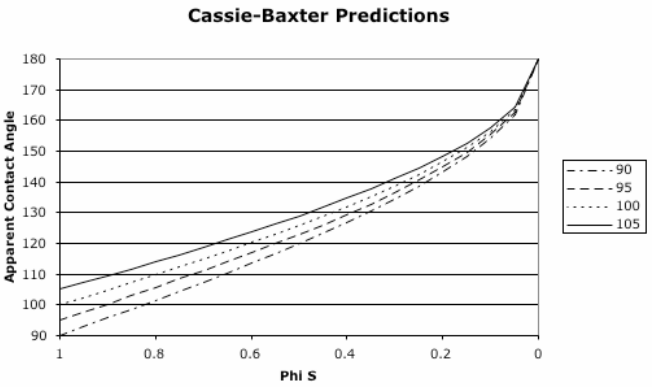

Figure 3 – Cassie-Baxter predictions for apparent contact angle as a function of the area fraction (ϕ_S).

After three days of curing the fractal surfaces reached their maximum apparent contact angle of 174°.

Another research group created highly ordered structures in 1999 using a combination of photolithography, sol-gel molding, and a hydrophobic surface coating [5]. The structure that yielded the largest contact angles was a rectangular array of one-micron posts and its contact angle was 170°. The data from this study fit the predictions of the Cassie-Baxter theory. Additionally, applying pressure to droplets on these surfaces forced a discontinuous jump to a reduced apparent contact angle of 130°, which matches the Wenzel predictions for complete wetting.

More recently, carbon nanotubes have been coated to form super hydrophobic surfaces with critical dimensions on the order of 50 nanometers [6]. The resulting surfaces have a contact angle near 170°. Again, this measurement is in agreement with the Cassie-Baxter predictions. However, the significant decrease in scale, thanks to the use of carbon nanotubes, makes this super hydrophobic surface much more robust than previous attempts. As mentioned above, droplets can be forced to completely wet the sol-gel surfaces. The carbon nanotube surface, on the other hand, is maintains the composite wetting condition even for a droplet falling onto the surface. Instead of completely wetting the surface and adhering, the droplet stays on top of the tubes, bounces, and eventually falls off the surface.

A research group at Bell Labs used electron beam (E-beam) lithography to create 350 nm diameter posts, which were coated to produce super hydrophobic surfaces [7]. The authors claimed to have a contact angle of "~180°," but their images and plots indicate actual numbers in the 170° range, similar to other super hydrophobic surfaces. This study was unique in that they were able to electronically switch the surface between complete and composite wetting conditions.

Clearly, the ability to change wetting conditions with surface structure has been demonstrated, but meaningful applications have yet to be thoroughly studied. One such application is the use of structured hydrophobic surfaces to reduce blood coagulation. It is well know that artificial materials that contact blood, either *in-vivo* or *ex-vivo*, are quickly subject to clot formation. The ability to resist blood clotting, or hemocompatibility, is a very valuable property for many medical devices such as stents, arterial grafts, and artificial heart valves. These devices are implanted in the body and exposed to blood, but hemocompatibility is important for devices that handle blood outside the body as well.

The clotting process is composed of an intricate sequence of chemical pathways [8]. Clotting is initiated by the activation of several proteins, Factor XII, Plasma prekallikrein, Factor XI, and High-molecular-mass kininogen (HMM-kininogen), when they come into contact with a foreign surface. Once the proteins are activated, a chemical chainreaction begins that results in the activation of platelets. Platelets then bind securely to the foreign surface where they attract and activate more platelets to form a clot. An important aspect of the clotting process is that the chemical reactions can only take place at the interface between the blood and foreign material.

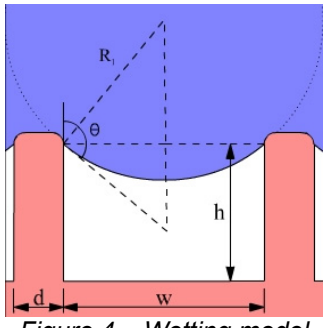

Figure 4 – Wetting model geometry.

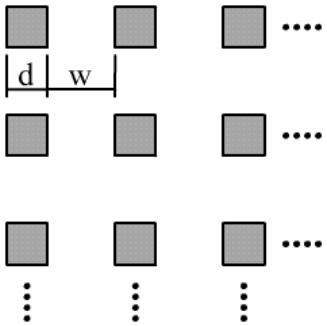

Figure 5 – Square posts, rectangular array.

3 THEORY

In order to use structured surfaces for hemocompatibility, it will be necessary to determine the wetting regime (composite or complete) in which the system is operating. A model can be developed from the simplified geometry shown in Figure 4. Surface tension is treated as a line force, so the fluid surface exerts a force tangent to its direction at the solid-liquid-vapor contact line and proportional to the length of the contact line. Again assuming vertical 1 dimensional features (ie. lines), the surface tension force can be resolved into the vertical direction as follows:

$$F_\gamma = -\gamma_{lv} \cdot l \cdot \cos(\theta) \tag{4}$$

where l is the length of the contact line. This can be converted into a pressure by dividing by the area of fluid that the force must support and multiplying by two because there is one force acting on each side of the area. In the one-dimensional case that area is $l \cdot w$, which results in a supportable pressure, ΔP, of:

$$\Delta P = \frac{-2 \cdot \gamma_{lv} \cdot \cos(\theta)}{w}. \tag{5}$$

Assuming that the features are square posts (Figure 5) with side lengths, d, the supportable pressure is

$$\Delta P = \frac{-4 \cdot \gamma_{lv} \cdot d \cdot \cos(\theta)}{w^2 + 2 \cdot d \cdot w}. \tag{6}$$

This result confirms the intuition from the 1-D structured case suggesting that the smaller the feature spacing the larger the pressure can be supported.

4 AXIOMATIC DESIGN OF BIOMEDICAL DEVICES

The goal of this research is to develop surfaces for use in biomedical devices. The Axiomatic Design [9] decomposition of a rather generic biomedical device is shown in Tab. 1 to illustrate where hemocompatible surfaces fit in the bigger picture.

	FRs	DPs
1	Perform specific device function	Device Specific Design
2	Prevent blood coagulation on device surfaces	Hemocompatible Surfaces
21	Reduce clotting reaction rates	Biochemical clotting deterrent
211	Chemically resist clotting at the blood-material interface	Controlled nitric oxide release
212	Maintain all blood and cell functions away from the device	Local anticoagulants only
22	Reduce blood-material	"Bed of nails" surface structure

	interaction	
221	**Reduce contact area, ϕ_S**	**Small ratio of critical dimension of the posts to space between posts, ε**
222	**Support specified blood pressure, (ΔP) with blood on top of the posts**	**Small space between posts, w**
23	**Reduce clotting reagent supply**	**Low platelet/clotting factor diffusion rate near the device**

Tab. 1 – AD device decomposition

This investigation focuses primarily on the geometric methods to reduce blood coagulation, so only the decomposition of DP22 is developed in detail, see [10] for full decomposition. DP22 decomposes to the following FRs:

FR221 = Reduce contact area, ϕ_S
FR222 = Support specified blood pressure, (ΔP) with blood on top of the posts

As in the Cassie-Baxter rough wetting theory, structure can only reduce the interaction between a fluid and the solid if the fluid is made to sit atop the posts (i.e. operate in the composite wetting regime). In this design, the blood must sit on top of the posts over the range of operating pressures for this device. FR222, support a specified blood pressure with the blood on top of the posts, is included to guarantee this behavior. Provided, that FR222 is satisfied, a reduction is surface area will clearly reduce the blood-material interaction. This is the motivation for FR221. This set of FRs can be satisfied by the following set of DPs:

DP221 = Small ratio of critical dimension of the posts to space between posts: $\varepsilon \equiv d/w$
DP222 = Small space between posts: w

This level of the design is characterized by the following design equation.

$$\begin{Bmatrix} FR221 \\ FR222 \end{Bmatrix} = \begin{bmatrix} X & 0 \\ X & X \end{bmatrix} \cdot \begin{Bmatrix} DP221 \\ DP222 \end{Bmatrix} \tag{7}$$

This is the leaf level of this decomposition branch, because we can now write algebraic equations in place of equation 7. Call the required blood pressure in FR222 ΔP and call the required area reduction (percent of previous area) in FR221 ϕ_S. As in Figure 4, call the space between the posts w and the critical dimension of the posts d. The critical dimension of the posts would be the diameter for circular posts, the side length for square posts, etc. As seen previously, the pressure that an array of square posts can support is given by the following equation:

$$\Delta P = \frac{-4 \cdot \gamma_{lv} \cdot d \cdot \cos(\theta)}{w^2 + 2 \cdot d \cdot w}. \tag{8}$$

This can be rewritten in terms of ε as:

$$\Delta P = \frac{-4 \cdot \gamma_{lv} \cdot \varepsilon \cdot \cos(\theta)}{w \cdot (1 + 2 \cdot \varepsilon)}. \tag{9}$$

FR222 is therefore a function of DP221 and DP222 and thus, equation 7 shows a coupling term between DP221 and FR222. From geometry, the area reduction, ϕ_S, delivered by a surface with square posts is

$$\phi_S = \left(\frac{\varepsilon}{\varepsilon + 1} \right)^2. \tag{10}$$

For circular posts the area reduction is

$$\phi_S = \frac{\pi}{4} \left(\frac{\varepsilon}{\varepsilon + 1} \right)^2. \tag{11}$$

FR221 is clearly a function of DP221 only and therefore, equation 7 shows that there is no coupling term between DP222 and FR221.

At this design level, another system constraint arises. The meniscus of the blood on top of the posts must not touch the bottom of the structure, or the structure will wet completely and FR222 will not be satisfied. This is incorporated into the design as a constraint (C3) on the aspect ratio (h/w) of the spaces between the posts. Assuming that the meniscus is a circular section, the aspect ratio of the spaces must be greater than some minimum value, AR_{min}.

$$AR_{\min} = \frac{1 - \sin\theta}{-2\cos\theta}. \tag{12}$$

5 MATERIALS AND METHODS

Photolithography offers the ability to carefully control geometry at the micron scale, so it is the obvious choice for creating structured test surfaces and molds. Moving to smaller scales with photolithography is possible for large-scale production, but it is too expensive and less robust in academic settings.

From the design decomposition above, it is clear that the desired geometry is a sparse arrangement of slender posts. The photoresist used for such features must be capable of relatively large aspect ratios and be strong enough to be used as part of the device or mold, rather than just as sacrificial layer for another process. The resist chosen for this task was SU-8 2000 (Microchem, Newton, MA). SU-8 2000 is a negative resist, so posts are made by exposing only the small sections that will become posts. If a positive resist were used, making posts with large spacing would require exposure of much more resist area, which could easily result in over-exposure.

To create SU-8 surfaces, three chrome on soda-lime photomasks (Advance Reproductions, North Andover, MA) were made, each with four 1-inch square patterned sections. Mask A has four patterns each with 20-μm square holes in the chrome. The four patterns are square arrays with area fractions (ϕ_S) of 4, 8, 12, and 16 percent. Mask B has two patterns with 15-μm square holes in the chrome and two with 25-μm square holes. The area fractions of the patterns for each hole size are 4 and 16 percent. Mask C has two patterns with 20-μm diameter circular holes and two patterns 20-μm wide lines. The circular patterns are square arrays of holes with periods of 100-μm and 50-μm. The patterns with lines are one-dimensional arrays of lines also with periods of 100-μm and 50-μm. SU-8 surfaces (Figure 6) are created from theses masks using contact photolithography.

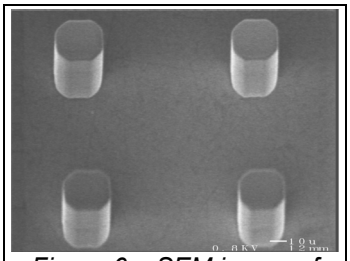

Figure 6 – SEM image of SU-8 surface with 20μm post and a designed ϕ_s of 0.04.

Poly-DimethylSiloxane (PDMS) was chosen as the material in which to fabricate test surfaces for the blood experiments. PDMS is used extensively in microfluidics and BioMEMS. It is popular because it can be quickly manufactured (curing times are about 2 hours, depending on the thickness of the PDMS) into working micro-scale devices. PDMS can be structured by casting features from a mold during curing in a furnace at 90°C. It has excellent feature replication allowing devices to be cast with critical dimensions well into the nanometer range. Additionally, PDMS is biocompatible and gas permeable making it an excellent candidate for biomedical devices. As cured, PDMS is a hydrophobic material (θ=107°) but oxidizing in air plasma can make PDMS hydrophilic.

The PDMS used in this study, Sylgard 184 (Dow-Corning, Midland, MI), is thoroughly mixed in a 10:1 base to curing agent ratio by mass. The mixture is degassed by placing it in a vacuum and periodically releasing the vacuum to burst the bubbles that rise to the top. The surface to be cast is cleaned with alcohol and then dried with nitrogen before being coated with a chemical release agent called (Tridecafluoro-1,1,2,2-tetrahydrooctyl) Tricholorosilane (Gelest Inc., Morrisville, PA). A few drops of the silane are placed into a vacuum desccator with the mold and a vacuum is drawn for ten minutes to fully silanize the surface. The PDMS mixture is poured over the silanized mold and everything is then placed back into a vacuum chamber to draw out any air that entered the mixture during pouring. The vacuum also ensures that the PDMS mixture completely fills in all the features of the mold. When all the gas has been removed, the mold and polymer are placed in an oven at 90°C and left for approximately two hours. Once cooled, the cured PDMS can be peeled from the mold and cut to size using a razor blade.

To create structured surfaces in PDMS based on the SU-8 surfaces, a double-casting method was used. The SU-8 surface was used as the original (positive image) mold and was cast to create a negative image, with holes as opposed to posts, of the structure in PDMS. This surface was then oxidized in air plasma for a minute before being used as a mold to cast a new layer of PDMS that has the original, positive image, of the SU-8 structure.

Testing the blood clotting process is challenging because it is triggered by a group of parallel protein reactions with many processes occurring simultaneously that are known collectively as contact activation. Since this investigation is meant to be a general investigation into the feasibility of the use of surface structure to improve hemocompatibility, it would be folly to focus specifically on any one of the paths or proteins involved in contact activation. Instead, it is advantageous to investigate the results of contact activation; that is the bonding of platelets to the surface and the continued agglomeration of platelets.

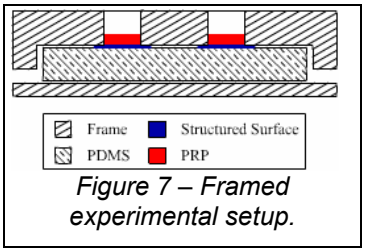

Figure 7 – Framed experimental setup.

This method is preferable because platelet deposition is much easier to measure than protein activation. Platelets are on the order of ~3μm in diameter, so they can be counted with a SEM microscope and the number can be compared to a control.

The first step in the experiment is to draw the blood from a donor using sodium citrate as an anticoagulant in the test tubes. The experiment must be completed within four hours from this point, because platelets stop functioning four hours after removal from the body. The blood is then placed in a centrifuge and spun at 1000 RPM for ten minutes to separate the platelet rich plasma from the rest of the blood. The platelet rich plasma is removed from the top of the centrifuge tubes and collected into one container. A hemocytometer is then used to measure the concentration of platelets in the plasma. A hemocytometer is basically a precision ground glass microscope slide with etched lines such that a known volume of liquid fits inside each square of etched lines. Platelet concentration can be measured by counting the number of platelets in several squares and then averaging.

Once the platelet concentration is known, the plasma is diluted to $1.5x10^5$ platelets/mm^3 using a phosphate buffer solution (PBS). The diluted plasma is applied to the surface being tested, incubated at 37°C for one hour before being washed off with PBS. The samples are soaked overnight in 2.5% gluteraldehyde and saline solution to fix the platelets that have adhered to the surface. The samples are dehydrated with ethanol and allowed to dry. They are then coated with 150Å of gold to allow for viewing in the SEM without surface charging.

Two experiments were run according to this procedure. In the first experiment, the platelet rich plasma was contained above the structured sections of the surface by a frame made out of low-density polyethylene (LDPE), shown in Figure 7. The LDPE frame must come in contact with the surface structure and the pressure applied to the frame to seal in the plasma deforms the structure as shown in Figure 8a. LDPE is a hydrophilic material, so the blood is drawn down into the structure at the edge (Figure 8b). From earlier experiments with water, it is clear that the composite wetting condition is only a meta-stable state of equilibrium. Once the fluid is allowed to touch the bottom of the valleys, the energy barrier between the composite wetting state and the complete wetting state is broken and the fluid completely wets the structure (Figure 8c).

In order to ensure that the composite wetting condition is maintained, the second experiment used drops of plasma instead of large amounts of plasma contained by the LPDE frame. The drops sit on top of the structure thanks to the slightly lower hydrostatic pressure and the lack of the LDPE frame pulling the fluid into the structure. The drops were placed in the center of each pattern. Smaller drops were used for the sparsest structure (ϕ_s=0.04) because large drops roll off the structure due to the slight inclination of the surface.

6 RESULTS

The first step in developing hemocompatible surface structure is ensuring that FR22 (Reduce blood-material interaction) is satisfied by the "bed of nails" surface structure (DP22). For practicality, this is done with water until the surfaces perform sufficiently well. The results are then verified with blood tests. This method assumes and then verifies that the fluid behavior of blood is similar to that of water because blood is composed mostly of water. As it turns out, blood and water have very similar contact angles with all the materials tested in this study.

Four SU-8 surfaces were created with designed area factions of 0.04, 0.08, 0.12, and 0.16 as described above. The actual surfaces had slightly large contact areas, but because the features were vertical posts, actual area fractions could be measured accurately using an optical microscope. The surfaces were coated with trichlorofluorosilane to give a flat surface contact angle of 103°. The actual contact areas along with the predicted and measured contact angles are shown in Tab. 2. It is clear that the data match pretty well with the predicted values. We can reasonably say from this that Cassie-Baxter theory holds for the geometries tested. Figure 9 shows a droplet on the flat coated surface next to a droplet on the surface with designed ϕ_s=0.04 to illustrate the magnitude of the change that can be attained simply by add surface structure.

In order to run the biological tests, the SU-8 Surfaces were used as molds to cast new surfaces in PDMS with the same geometry, but with a flat surface contact angle of 107°. These surfaces also performed well with respect to the Cassie-Baxter predictions (Figure 10, Tab. 2). The difference between the SU-8 and the PDMS structures cannot be fairly compared due the limitations of the measurement technique.

Surface	Designed ϕ_s	Measured ϕ_s	Flat Surface Contact Angle	Cassie Predicted	Measured
SU-8 with	0.04	0.06	103°	162°	160°
Silane Coating	0.08	0.12	103°	154°	150°
	0.12	0.18	103°	149°	145°
	0.16	0.25	103°	143°	130°
PDMS Casts of SU-8	0.04	0.06	107°	163°	160°
	0.08	0.12	107°	156°	145°
	0.12	0.18	107°	150°	140°
	0.16	0.25	107°	145°	130°

Tab. 2 – Apparent Contact Angle Experimental Results

Figure 11 shows a typical control sample from the first blood interaction experiment (with frame). The platelets are the 2-μm bumps that dot the surface and often appear white around the edges. Figure 12 is a typical SEM image of the PDMS surface that has an area fraction (ϕ_s) of 12 percent and Figure 13 is a typical image of a surface with an area fraction (ϕ_s) of 16 percent. Clearly, these surfaces are not an improvement on the flat surface.

Recall from earlier that the 16 percent area fraction surfaces, because of their small inter-post spacing, were the most robust in preventing water from completely wetting the surface. Consequently, it would follow that they would be the most likely surfaces to show a reduction in coagulation. Interestingly, the surface with an area fraction of (ϕ_s) 4 percent Figure 14 seems to perform better than the denser surfaces that were more robust in early tests. It seems that the tops of the posts on the sparse structure have fewer platelets than an equal area of from the control sample, yet the spaces between the posts have more platelets than the control surfaces. The hypothesis was that the sparser surfaces would perform better, than the dense surfaces and that all of the structured surfaces would perform better than the flat surfaces. The apparent rearranging of the performance hierarchy from that of the hypothesis has especially troubling implications for the original motivation of reducing blood fouling by reducing contact area. Fortunately, the problem was a result of operating in the complete wetting condition as described above.

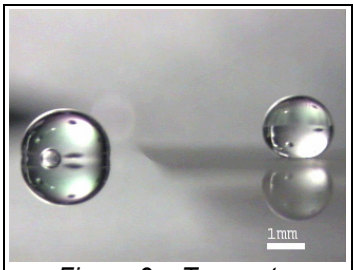

Figure 9 – Two water droplets one on a flat silanized SU-8 surface (left) and one on a structured silanized SU-8 surface (right).

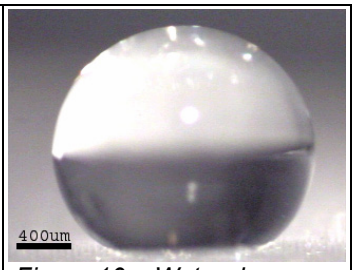

Figure 10 – Water drop on a PDMS surface with ϕ_s=0.04.

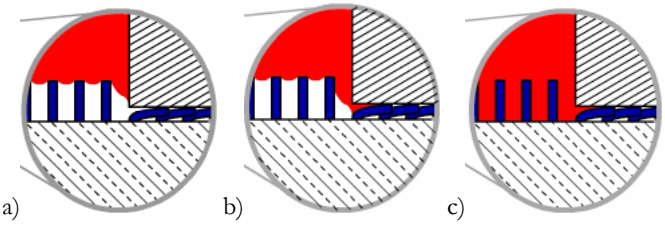

Figure 8 – Failure mode for first blood experiment.

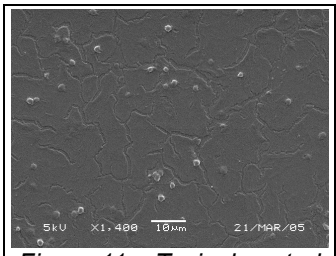

Figure 11 – Typical control sample tested with frame.

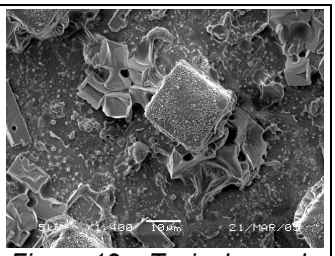

Figure 12 – Typical sample with ϕ_s=0.12 tested with frame.

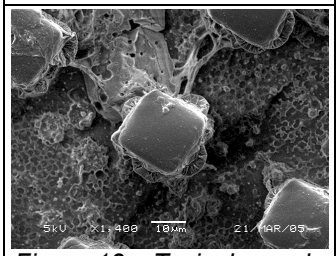

Figure 13 – Typical sample with ϕ_s=0.16 tested with frame.

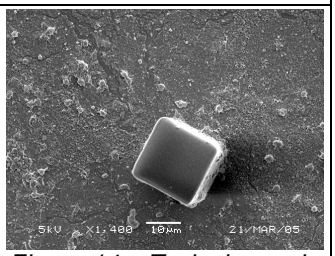

Figure 14 – Typical sample with ϕ_s=0.04 tested with frame.

Figure 15 shows a typical SEM image of the flat surface control from the second experiment design to operate in the composite wetting condition. The control samples in both experiments are very similar, suggesting that the application of the plasma in drop form or in the frame does not seriously influence platelet deposition. Figure 16, Figure 17, Figure 18 and Figure 19 show typical SEM images from the surfaces with area fraction of 4, 8, 12, and 16 percent, respectively. The tops of the posts for the 4 percent area fraction surface are clearly very clean; several of the images show a platelet on the top of the posts, but most are completely clear. SEM images focused at the base of the posts, Figure 20, show some debris and the occasional platelet, but significantly less build up than in the previous experiment. The denser patterns show slight increases in platelet adhesion on the tops of the posts with little change in the build up at the base of the posts. There was a large jump in platelet deposition on the top of the posts from the 12 percent area fraction to the 16 percent area fraction.

The first experiment shows that an increase in contact area between the blood and the surface increases platelet accretion and general surface fouling. The results of the second experiment show that the reduction in contact area between the blood and the surface does reduce platelet accretion. Despite the apparent failure of the first experiment, it provided extra support for the central hypothesis.

The goal of these blood tests was to quantify the change in platelet adhesion between flat and structured PDMS surfaces. However, several factors involved in the experiments make any quantitative assertions suspect. For instance, the blood used in each of the two tests came from different subjects. Even though the platelet rich plasma was adjusted to a specified platelet concentration differences between samples could still skew the results. Furthermore, only one surface sample was used in each test and the area eventually cut out and examined in the SEM was fairly small. Dirt or other local anomalies in the samples could affect the results. Consequently, only qualitative results can be taken from these experiments as initial proof of concept.

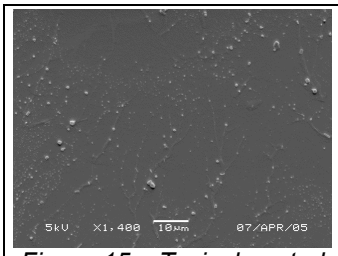

Figure 15 – Typical control sample tested with a drop.

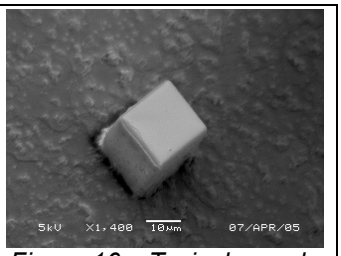

Figure 16 – Typical sample with ϕ_s=0.04 tested with a drop.

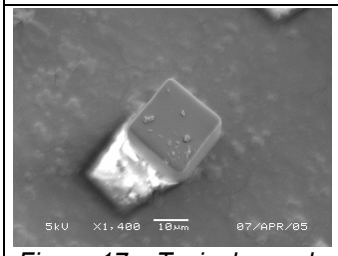

Figure 17 – Typical sample with ϕ_s=0.08 tested with a drop.

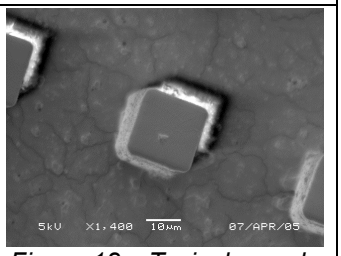

Figure 18 – Typical sample with ϕ_s=0.12 tested with a drop.

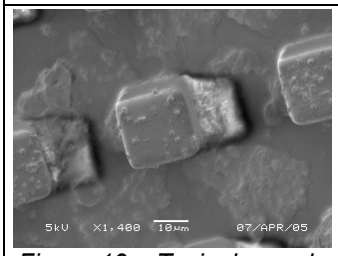

Figure 19 – Typical sample with ϕ_s=0.16 tested with a drop.

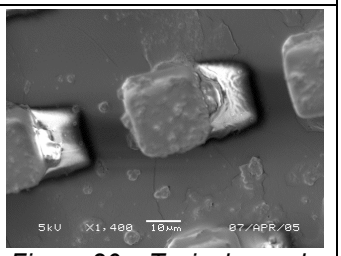

Figure 20 – Typical sample with ϕ_s=0.16 tested with a drop with image focused at the base of the posts.

7 CONCLUSIONS

Superhydrophobic surfaces are designed such that they meet the two requirements to support a fluid pressure and to reduce contact area between the fluid and the surface. These surfaces are fabricated in both rigid and flexible materials and their superhydrophobic performance is verified with apparent contact angles of 160°. It is postulated that such structutred surfaces should be able to reduce the clotting of blood by reducing available contact area.

The surfaces are tested for platelet clotting and show improvement in performance for surfaces with a critical dimension of 20µm with static fluid *in-vitro*. Platelet rich plasma (PRP) left on structured surfaces of polydimethylsiloxane (PDMS) at body temperature for a fixed time results in noticeably less platelet adhesion than the case for PRP left on flat PDMS for the same period. The platelet adhesion results are achieved qualitatively by examining scanning electron microscope (SEM) images of the tested surfaces. The qualitative results are

encouraging enough to warrant further study with more precise experiments that could yield quantitative results for confirmation of the mechanisms driving the apparent reduction in platelet adhesion.

8 REFERENCES

[1] Wenzel, R.N. "Resistance of Solid Surfaces to Wetting by Water." *Industrial and Engineering Chemistry* 28 (1936): 988-994.

[2] Wenzel, R.N. "Surface Roughness and Contact Angle." *Journal of Physical Colloid Chemistry* 53 (1949): 1466-1467.

[3] Cassie, A.B.D. and Baxter, S. "Wettability of Porous Surfaces," *Transactions of the Faraday Society* 40 (1944): 546-551.

[4] Shibuichi, Satoshi, et al. "Super Water-Repellent Surfaces Resulting from Fractal Structure." *Journal of Physical Chemistry* 100 (1996): 19512-19517.

[5] Bico, J., Marzolin, C., and Quere, D. "Pearl Drops." *Europhysics Letters* 47 (1999): 220-226.

[6] Lau, Kenneth, et al. "Super hydrophobic Carbon Nanotube Forests." *Nano Letters* 3 (2003): 1701-1705.

[7] Krupenkin, Tom, et al. "From Rolling Ball to Complete Wetting: The Dynamic Tuning of Liquids on Nanostructured Surfaces." *Langmuir* 20 (2004): 3824-3827.

[8] Halkier, Torben. *Mechanisms in Blood Coagulation Fibrinolysis and the Complement System.* Trans. Paul Woolley. Cambridge: Cambridge University Press, 1991.

[9] Suh, N.P. *Axiomatic Design: Advances and Application.* New York: Oxford University Press, 2001.

[10] Schrauth, A.J. *Structured Surfaces for Hemocompatibility.* Massachusetts Institute of Technology: Masters Thesis, 2005.